Geometrically and Conformationally Restrained Cinnamoyl Compounds as Inhibitors of HIV-1 Integrase: Synthesis, Biological Evaluation, and Molecular Modeling

Marino Artico,*,† Roberto Di Santo,† Roberta Costi,† Ettore Novellino,‡ Giovanni Greco,§ Silvio Massa,|| Enzo Tramontano,⊥ Maria E. Marongiu,⊥ Antonella De Montis,⊥ and Paolo La Colla*,⊥

Istituto Pasteur - Fondazione Cenci Bolognetti, Dipartimento di Studi Farmaceutici, Università di Roma "La Sapienza", Piazzale A. Moro 5, I-00185 Roma, Italy, Dipartimento di Scienze Farmaceutiche, Università di Salerno, Piazza Vittorio Emanuele 9, I-84084 Penta (Salerno), Italy, Dipartimento di Chimica Farmaceutica e Tossicologica, Università di Napoli "Federico II", Via D. Montesano 49, I-80131 Napoli, Italy, Dipartimento Farmaco Chimico Tecnologico, Università di Siena, Banchi di Sotto 55, I-53100 Siena, Italy, and Dipartimento di Biologia Sperimentale, Università di Cagliari, Viale Regina Margherita 45, I-09124 Cagliari, Italy

Received October 23, 1997

Various cinnammoyl-based structures were synthesized and tested in enzyme assays as inhibitors of the HIV-1 integrase (IN). The majority of compounds were designed as geometrically or conformationally constrained analogues of caffeic acid phenethyl ester (CAPE) and were characterized by a syn disposition of the carbonyl group with respect to the vinylic double bond. Since the cinnamoyl moiety present in flavones such as quercetin (inactive on HIV-1-infected cells) is frozen in an anti arrangement, it was hoped that fixing our compounds in a syn disposition could favor anti-HIV-1 activity in cell-based assays. Geometrical and conformational properties of the designed compounds were taken into account through analysis of X-ray structures available from the Cambridge Structural Database. The polyhydroxylated analogues were prepared by reacting 3,4-bis(tetrahydropyran-2-yloxy)benzaldehyde with various compounds having active methylene groups such as 2-propanone, cyclopentanone, cyclohexanone, 1,3-diacetylbenzene, 2,4-dihydroxyacetophenone, 2,3-dihydro-1-indanone, 2,3-dihydro-1,3-indandione, and others. While active against both 3′-processing and strand-transfer reactions, the new compounds, curcumin included, failed to inhibit the HIV-1 multiplication in acutely infected MT-4 cells. Nevertheless, they specifically inhibited the enzymatic reactions associated with IN, being totally inactive against other viral (HIV-1 reverse transcriptase) and cellular (RNA polymerase II) nucleic acid-processing enzymes. On the other hand, title compounds were endowed with remarkable antiproliferative activity, whose potency correlated neither with the presence of catechols (possible source of reactive quinones) nor with inhibition of topoisomerases. The SARs developed for our compounds led to novel findings concerning the molecular determinants of IN inhibitory activity within the class of cinnamoyl-based structures. We hypothesize that these compounds bind to IN featuring the cinnamoyl residue C═C−C═O in a syn disposition, differently from flavone derivatives characterized by an anti arrangement about the same fragment. Certain inhibitors, lacking one of the two pharmacophoric catechol hydroxyls, retain moderate potency thanks to nonpharmacophoric fragments (i.e., a *m*-methoxy group in curcumin) which favorably interact with an "accessory" region of IN. This region is supposed to be located adjacent to the binding site accommodating the pharmacophoric dihydroxycinnamoyl moiety. Disruption of coplanarity in the inhibitor structure abolishes activity owing to poor shape complementarity with the target or an exceedingly high strain energy of the coplanar conformation.

Introduction

Monotherapy with available drugs, which target the retroviral enzymes reverse transcriptase (RT)[1] and protease (PR),[2] has failed to provide long-term suppression of HIV-1 replication in infected individuals. To obtain a more effective treatment of AIDS, efforts are actually directed toward the design of combination therapies and the exploitation of new targets.[3]

In addition to RT and PR, another target potentially amenable to a selective chemotherapeutic intervention is the HIV-1 integrase (IN), an enzyme which has no counterparts in the host cell and catalyzes an essential step in the retroviral life cycle.[4,5] In fact, following reverse transcription of the viral DNA genome into a double-stranded DNA (dsDNA), IN catalyzes integration of the latter into the host chromosome through coordinated reactions of processing and joining.[6] Initially the enzyme recognizes the LTR termini of the viral dsDNA, of which it removes the last two nucleotides (GT) leaving two recessed 3′-OH ends. Then, IN catalyzes joining of the processed viral 3′-ends to the 5′-ends of strand breaks in the host DNA. Removal of mispaired nucle-

* Corresponding authors.
† Università di Roma "La Sapienza".
‡ Università di Salerno.
§ Università di Napoli "Federico II".
|| Università di Siena.
⊥ Università di Cagliari.

S0022-2623(97)00723-1 CCC: $15.00
Published on Web 09/17/1998

Chart 1. HIV-1 Integrase Inhibitors

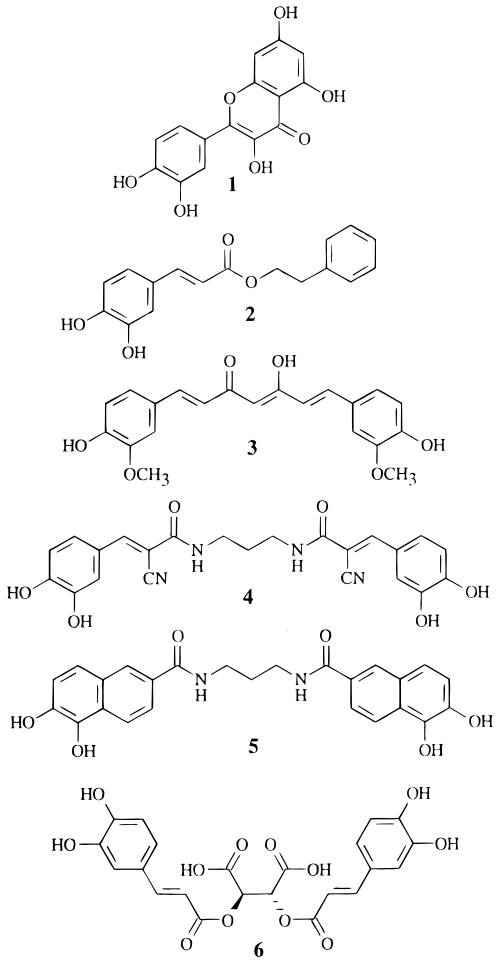

otides and gap repair, which are carried out by cellular enzymes, leads to provirus formation.[7]

Many different classes of compounds have been reported to inhibit the HIV-1 IN in enzyme assays, and among them, natural and synthetic polyhydroxylated molecules have emerged as potent IN inhibitors (Chart 1). They include flavones such as quercetin (**1**),[8] caffeic acid phenethyl ester (CAPE) (**2**) and related amides,[8,9] bis-catechols,[10] curcumin (**3**),[11] a tyrphostin (**4**) and its potent 6,7-dihydroxynaphtho-2-yl derivative (**5**),[12] (−)-arctigenin,[13] and L-chicoric (**6**) and dicaffeoylquinic acids.[14] However, very few of the above compounds have shown specific anti-IN activity, and still fewer proved active in cell-based assays. Notable exceptions are L-chicoric acid and some dicaffeoylquinic acids isolated from Bolivian medicinal plants which, in addition to being very potent and specific IN inhibitors in enzyme assays, inhibit the HIV-1 multiplication in acutely infected cells at noncytotoxic concentrations.[14] Interestingly, the latter compounds are characterized by a 3,4-dihydroxycinnamoyl moiety which is also present in most of the above IN inhibitors, sometimes incorporated in a ring structure as in quercetin and 6,7-dihydroxynaphtho-2-yltyrphostin. The only other polyhydroxylated IN inhibitor which has been reported moderately active in cell-based assays is curcumin,[15] a pigment isolated from the rhizomes of *Curcuma longa*, which exhibits a variety of pharmacological properties, antiinflammatory and antitumor activities included. However, the low potency of curcumin can be likely

Chart 2. Cinnamoyl-Based Derivatives Investigated as IN Inhibitors

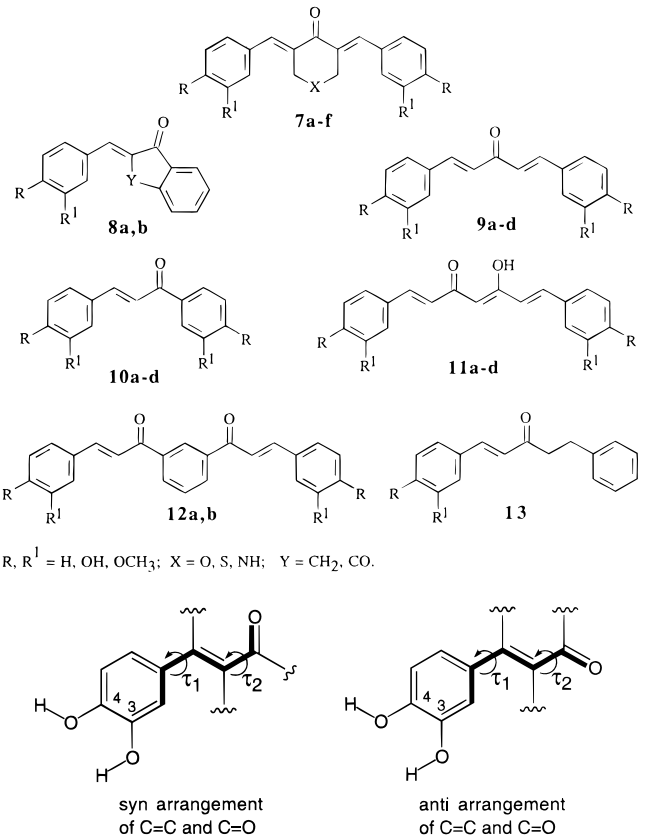

Figure 1. Torsional angles τ_1 and τ_2 for 3,4-dihydroxycinnamoyl-like structures are defined by thick lines. Syn and anti mutual dispositions of C=C and C=O groups correspond to τ_2 values of about 0° and 180°, respectively.

ascribed to the presence of an *o*-methoxyhydroxy, rather than the *o*-dihydroxy system which is known to correlate with potent anti-IN activity.

Although the 3D structure of HIV-1 IN has been partly solved by X-ray crystallography,[16] target structure-based design of novel inhibitors is currently hampered by the fact that one of the most important domains of this enzyme, namely, the one containing the catalytic residue Glu-152, has been found disordered to such a great extent that its structure could not be determined. Therefore, design of novel IN inhibitors and interpretation of structure−activity relationships (SARs) for this class of compounds are still ligand structure-based.

With the aim of obtaining more potent anti-IN inhibitors, hopefully active also in HIV-1-infected cells, we synthesized various polyhydroxylated cinnamoyl-containing derivatives (**7**−**13**) (Chart 2) and tested them for activity against HIV-1 IN, RT, and cellular RNA polymerase in enzyme assays as well as for anti-HIV-1 antiproliferative and antitopoisomerase activity in cell-based assays.

Most of our compounds were designed as geometrically or conformationally constrained cinnamoyl structures characterized by a syn disposition of the carbonyl group with respect to the vinylic double bond (Figure 1). The rationale of "freezing" the C=C−C=O moiety in a syn arrangement relied on the observation that flavones such as quercetin (**1**) are inactive on HIV-1-infected cells (in all of them the C=C−C=O fragment

Scheme 1

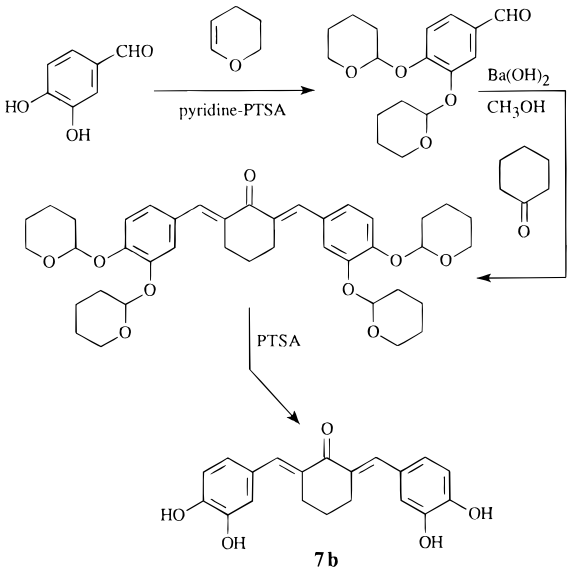

is geometrically fixed in anti) whereas some flexible CAPE derivatives, like L-chicoric acid (**6**), display anti-HIV-1 activity in cultured cells. It was hoped that stabilization of the syn arrangement in CAPE analogues, through geometrical (bond connectivity) or conformational constraints, could yield novel IN inhibitors effective in cell-based assays. The design of the new inhibitors was assisted by analysis of X-ray structures retrieved from the Cambridge Structural Database (CSD)[17] of compounds coincident or congeneric with those synthesized and tested.

Chemistry

Curcumin and related compounds **11a**−**d** were prepared according to Babu and Rajasekharan by condensation of the proper arylaldehyde with acetylacetone and boric acid in the presence of 1,2,3,4-tetrahydroquinoline.[18] For the synthesis of the other arylidene derivatives, the use of 3,4-dihydroxybenzaldehyde required preventive protection of the hydroxyl groups of the catechol system, preferably with easily removable groups such as tetrahydropyran-2-yl.[19] We therefore reacted 3,4-dihydroxybenzaldehyde with 3,4-dihydro-α-pyran in the presence of pyridinium *p*-toluenesulfonate to achieve 3,4-bis(tetrahydropyran-2-yloxy)benzaldehyde (Scheme 1).

Polyhydroxylated derivatives were then prepared by reacting 3,4-bis(tetrahydropyran-2-yloxy)benzaldehyde with various compounds having active methylene groups such as 2-propanone, cyclopentanone, cyclohexanone (reported in Scheme 1 as a representative example of the general procedure), 1,3-diacetylbenzene, 2,4-dihydroxyacetophenone, 2,3-dihydro-1-indanone, 2,3-dihydro-1,3-indandione, and others. Condensation was carried out in alkaline medium according to the published procedure.[20]

The crude chalcone-like derivatives obtained from condensation were subjected to deprotection by hydrolytic cleavage in the presence of *p*-toluenesulfonic acid as a catalyst. This procedure was used for achieving the mono- and bis-arylidene derivatives **7**−**13** described in Tables 1 and 2, whereas 3,5-bis(3,4-dihydroxybenzylidene)piperidin-4-one (**7f**) was easily obtained by

Scheme 2

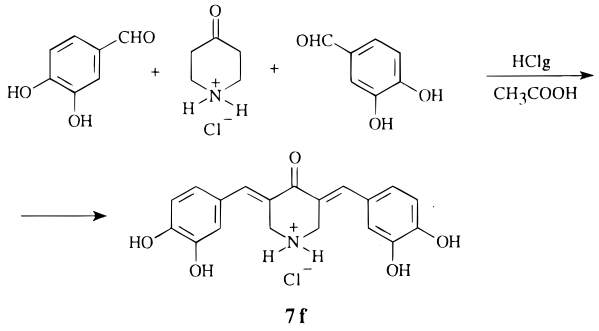

reacting 3,4-dihydroxybenzaldehyde with piperidin-4-one hydrochloride in glacial acetic acid under a stream of gaseous hydrochloric acid (Scheme 2).

Results and Discussion

Molecular Design. As stated, analysis of crystal structures retrieved from the Cambridge Structural Database (CSD)[16] allowed us to take into account geometrical and conformational features of the designed compounds. These were synthesized and tested in order to address the following SAR issues.

The effect of constraining in a syn disposition the C=C and C=O fragments of the cinnamoyl chain (Figure 1) was evaluated by synthesis of the geometrically constrained cyclovalone analogues **7a**−**f** and indan derivatives **8a**,**b**. Compounds **9a**−**d**, forced into a syn arrangement by conformational factors, were synthesized as open-chain counterparts of **7a**−**f**. Through **7a**−**f** and **9a**−**d** we also investigated symmetrical cinnamoyl moieties sharing the same carbonyl group. Chalcone derivatives **10a**−**d**, stable as syn conformers, represented a further step toward molecular simplification as they formally result from removal of one of the two vinylic moieties in compounds **9a**−**d**.

Effects on anti-IN activity related to an increased distance between the two terminal aromatic moieties were evaluated by synthesis of curcumin analogues **11a**−**d** and especially of 1,3-bis(cinnamoyl)benzene derivatives **12a**,**b**. In these molecules, both syn and anti conformations are energetically feasible.

Preparation and testing of **13**, which cannot attain a fully coplanar conformation, provided information concerning shape-dependent effects relevant to IN inhibitory activity.

A correlation has been repeatedly found between the anti-IN potency of polyhydroxylated aryl compounds and the number and/or mutual positioning of hydroxyl groups, the most active compounds being those containing two pairs of *o*-bis-hydroxy substituents.[21] To verify whether such a pattern held likewise in our series, so as to support a mechanism of action similar to that of other CAPE analogues, the designed compounds differed also in the number of free hydroxyl groups.

Anti-IN Assays. All the synthesized compounds were initially tested in a dual 3′-processing and strand-transfer assay together with aurintricarboxylic acid (ATA), used as reference compound.[22] In this study, a purified HIV-1 IN expressed in *Escherichia coli* was incubated with a 21-mer double-stranded oligonucleotide corresponding to the U5 end of the HIV-1 LTR, labeled at the 3′-end of the plus strand. This allowed a

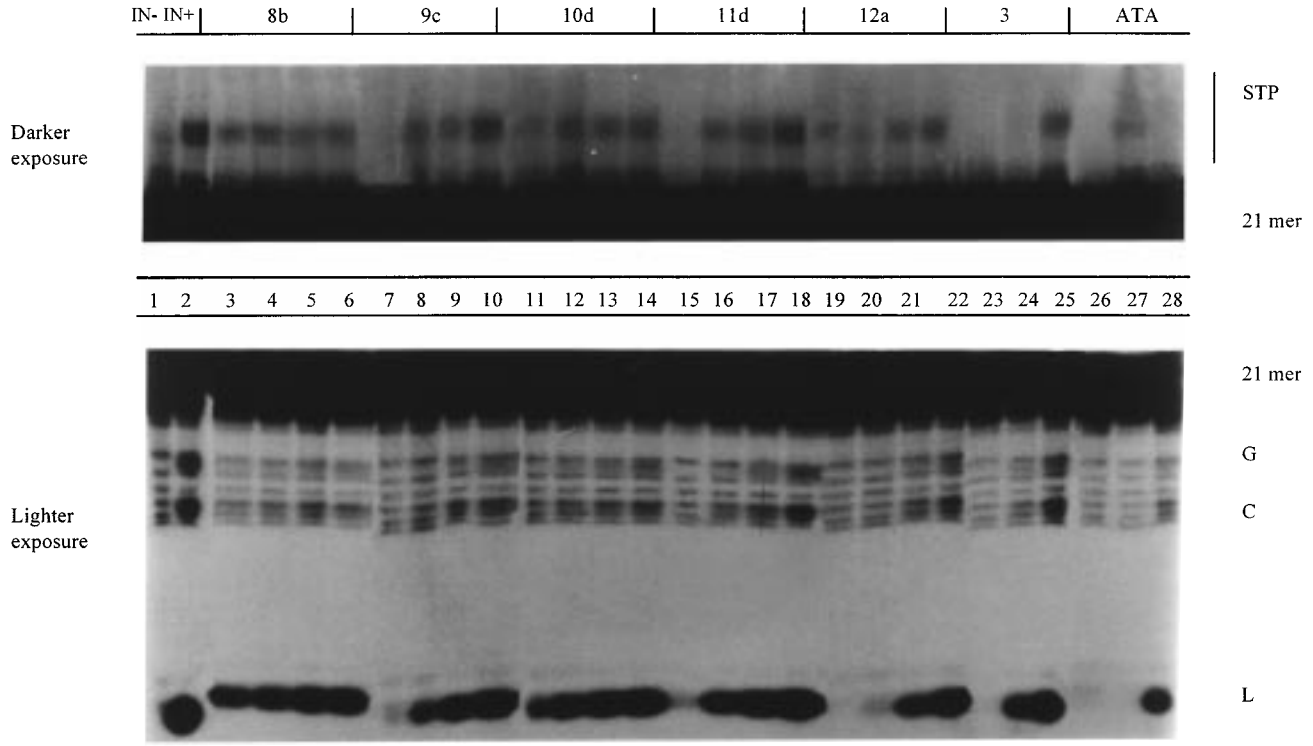

Figure 2. Inhibition of HIV-1 IN-catalyzed 3′-processing and strand-transfer reactions by curcumin and related derivatives. The DNA strand-transfer products (upper pannel) migrate more slowly than 21-mer substrate and 3′-processing products G, C, and L (lower panel). The upper panel is a darker exposure of the gel in order to show the integration products. Lane 1, without DNA; lane 2, +IN without drugs; lanes 3−6, with **12b** (100, 50, 25, 12.5 μM); lanes 7−10, with **9c** (1.2, 0.6, 0.3, 0.15 μM); lanes 11−14, with **7d** (0.6, 0.3, 0.15, 0.07 μM); lanes 15−18, with **10d** (10, 5, 2.5, 1.2 μM); lanes 19−22, with **8a** (10, 5, 2.5, 1.2 μM); lanes 23−25, with **3** (50, 25, 12.5 μM); lanes 26−28, with ATA (1.2, 0.6, 0.3 μM).

rapid and quantitative recovery, by gel filtration, of the acid-soluble dinucleotides released by IN in the 3′-processing reaction and, thus, a very accurate comparison of the anti-IN potencies of test compounds. On the other hand, separation of reaction products by denaturing PAGE and densitometric quantification allowed us to measure the extent of inhibition of both 3′-processing and strand-transfer reactions. A typical experiment is shown in Figure 2.

The IC_{50} values presented in the SAR study of Table 2 refer to 3′-processing reactions analyzed by gel filtration. However, it should be noted that essentially similar IC_{50} values were obtained when: (a) 3′-processing and strand-transfer reactions were monitored by PAGE and densitometric quantification; (b) the strand-transfer reaction was carried out with a 5′-labeled substrate (see Experimental Section) corresponding to the product of the 3′-processing reaction (data not shown).

Sequence-specific removal of the labeled terminal dinucleotide by intervention of nucleophiles, such as glycerol, 3′-OH groups of the substrate DNA, and water, generates 5′-glycerol-phosphate-GT_{OH} (G), cyclic-GT (C), and 5′-phosphate-GT_{OH} (L), respectively, as reaction products.[23] When formation of the latter was analyzed by denaturing PAGE gels, like those illustrated in Figure 2, all the active compounds were found to inhibit the 3′-processing reaction in a dose-dependent manner (lower panel). Moreover, the fact that our compounds inhibited the formation of G, C, and L to the same extent suggested that all of them blocked nucleophilic attack, likely binding at the IN active site.

Table 1. Chemical and Physical Data of Derivatives **7**−**13**

compd	mp (°C)	recrystn[a] solvent	yield (%)	reaction time (h)	chromat[b] system	ref
7a	179−181	a	22	0.5		33
7b	244−246	b	99	7	A	40
7c	>300	b	42	1	B	41
7d	>300	c	46	3.5	B	
7e	223−225	d	98	1	B	
7f	>300	e	92	48		
8a	262−264	c	53	4		42
8b	264−266	c	56	3		
9a	68−70	e	64	1	C	43
9b	114−116	e	18	72	C	44
9c	221−223	f	24	2	D	
9d	248−250	c	74	2		45
10a	212−214	c	66	15	E	46
10b	232−234	c	39	19[c]	E	47
10c	209−210	a	93	12	F	19
10d	199−201	d	100	15	G	48
11a	128−130	e	55	4		18
11b	193−195	g	10	4	H	20
11c	216−218	h	26	4	H	49
11d	136−137	i	19	4	C	50
12a	>300	c	48	4	A	
12b	210−211	c	26	4	I	
13	160−162	f	24	6	A	

[a] Recrystallization solvents: a, acetic acid; b, methanol/water; c, methanol; d, tetrahydrofuran/toluene; e, ethanol; f, ethanol/toluene; g, toluene; h, toluene/benzene; i, cyclohexane. [b] Chromatographic system silica gel: A, chloroform/methanol, 20:1, B, chloroform/methanol; C, chloroform; D, chloroform/ethyl acetate, 1:1; E, diethyl ether/*n*-hexane, 1:1; F, diethyl ether/*n*-hexane, 3:2; G, diethyl ether/*n*-hexane, 2:1; H, chloroform/ethyl acetate, 9:1; I, chloroform/methanol, 20:1. [c] Reflux time.

A longer exposure of the gel (Figure 2, upper panel) allowed us to see that active compounds also inhibited the strand-transfer reaction in a dose-dependent man-

Table 2. Structures and Biological Properties of Cinnamoyl-Based Derivatives

compd	Formula	IC_{50}[a] 3'-processing	CC_{50}[b] MT-4	CC_{50}[b] KB	PLDB[c] fold increase
7a	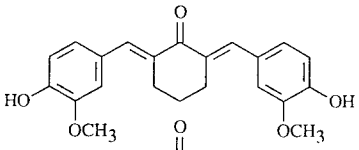	>100	2.4	6.7	1.8 ± 0.5
7b	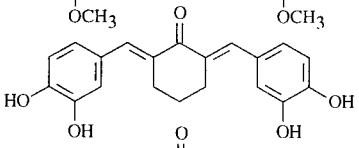	0.9±0.1	7.4	8.9	1.4 ±0.5
7c	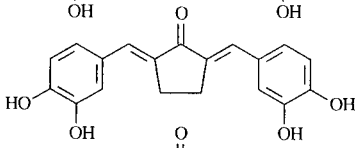	1±0.2	15	17	4.0 ± 1.0
7d	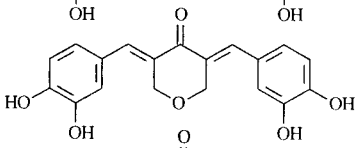	0.2±0.1	10	15	0.9 ± 0.1
7e	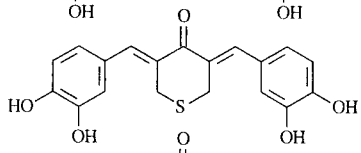	0.2±0.1	4	3.9	1.1 ± 0.1
7f	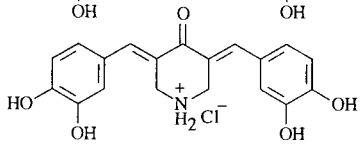	0.2±0.03	21	32	1.4 ± 0.2
8a	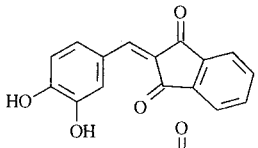	3±0.5	32	50	2.0 ± 0.4
8b	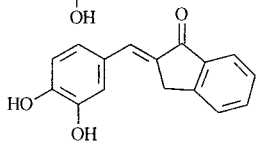	86 ± 5	5.5	9.2	5.1 ± 1.0
9a	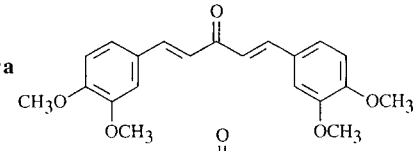	>100	4.1	6.7	1.1 ± 0.2
9b	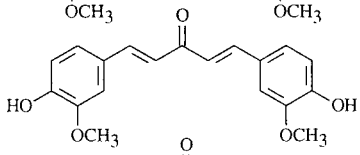	37 ± 15	1.4	8.5	1.2 ± 0.3
9c	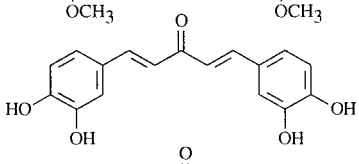	0.6±0.3	38	21	1.1 ± 1.0
9d	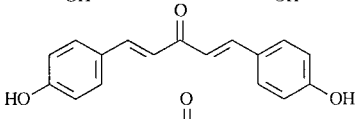	>100	1.6	7.4	1.1 ± 0.5
10a	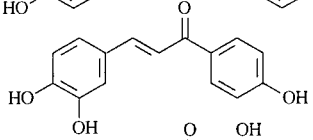	1.3±0.6	4.4	5.9	1.6 ± 0.5
10b	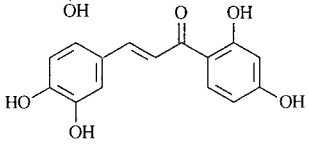	20±4	5.3	9.1	2.2 ± 0.6

Table 2 (Continued)

compd	Formula	IC_{50}[a] 3′-processing	CC_{50}[b] MT-4	CC_{50}[b] KB	PLDB[c] fold increase
10c	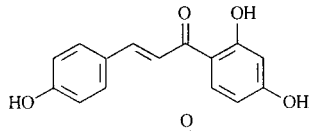	>100	7.4	12	1.7 ± 0.1
10d	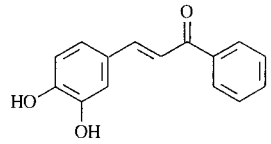	2.3±0.9	1.7	3.1	1.3 ± 0.2
11a	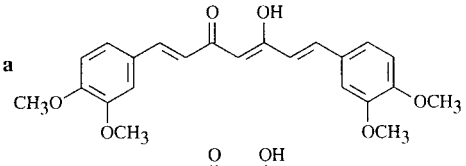	>100	4.1	2.0	1.4 ± 0.1
11b	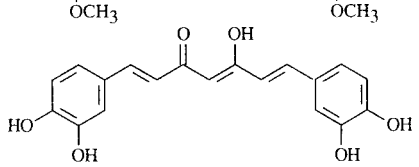	0.7 ± 0.3	17	4.1	1.1 ± 0.5
11c	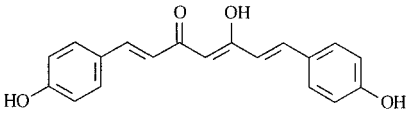	>100	13	8.5	0.9 ± 0.2
11d	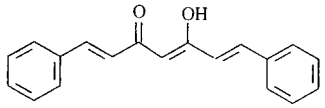	>100	41	29	0.8 ± 0.02
12a	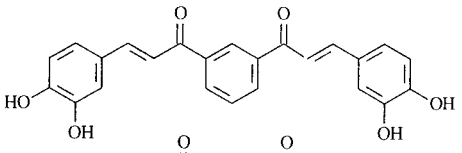	0.8 ± 0.2	5.0	5.8	1.2 ± 1.0
12b	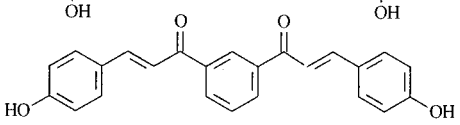	30 ± 10	35	22	1.2 ± 0.5
13	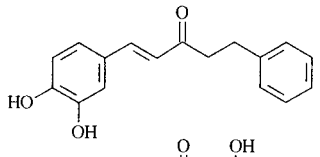	>100	15	30	1.0
3 Curcumin	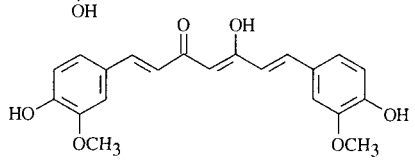	30 ± 6	7.4	16	1.0 ± 0.1
VP-16		>100	0.08	0.1	11 ± 2.0
CPT		>100	0.01	0.006	3.5 ± 1.2
ATA[d]		0.17 ± 0.02	42.2	42.2	1.1

[a] Compound concentration (μM) required to reduce HIV-1 IN 3′-processing activity by 50%. Data represent mean values ± SD for three independent determinations. [b] Compound concentration (μM) required to reduce the exponential growth of MT-4/KB cells by 50%. [c] Fold increase in protein-linked DNA breaks (PLDB) with respect to untreated controls. Compound concentrations were 10 × CC_{50} for KB cells. [d] CC_{50} and IC_{50} are expressed as μg/mL.

ner, as evidenced by a decrease in the amount of larger reaction products.

IN Inhibitory Activities. The IC_{50} values listed in Table 2 range from 0.2 to above 100 μM (threshold value for compounds considered inactive). The highest potency was obtained with cyclovalone analogues **7b**−**f** in

which the symmetric dihydroxycinnamoyl chains are fixed in a syn arrangement (Figure 1).

Methylation of the two *m*-hydroxyls in **7b** yielded **7a** which is devoid of activity. Compounds **9a**−**d**, open-chain analogues of the cyclovalone compounds, displayed submicromolar activity when the bis-catechol moieties were preserved (**9c**); otherwise activity decreased (**9b**) or was lost (**9a**,**d**). Indan derivatives **8a**,**b**, both geometrically constrained in a syn disposition, turned out active and moderately active, respectively. Chalcones **10a**,**d**, featuring a single *o*-hydroxycinnamoyl residue, exhibited good activity. Hydroxylation of **10a** at the position ortho to the carbonyl group, so as to give **10b**, caused a significant drop of activity. Lack of the catechol system in the chalcone series, as in **10c**, destroyed activity. Examination of anti-IN activity values within the series of curcumin (**11a**−**d**) and 1,3-bis(cinnamoyl)benzene (**12a**,**b**) derivatives revealed that activity required the presence of *o*-hydroxyls (**11b** and **12a**), whereas activity was relatively independent of the distance between the catechol units and the nature of the central linker. Compound **13**, the only one in our set predicted noncoplanar by molecular modeling analysis, resulted totally inactive.

Antiretroviral Effect. Since curcumin has been reported[15] active against the HIV-1 multiplication in cell-based assays, we tested our inhibitors for their capability to selectively inhibit the HIV-1-induced cytopathic effect (CPE) in de novo infected MT-4 cells. However, under conditions where nevirapine and AZT, which were used as reference compounds, showed EC_{50}'s of 0.01 and 0.25 μM, respectively, curcumin was unable to prevent the virus-induced CPE. Similarly, none of the compounds under investigation inhibited the HIV-1 multiplication at concentrations below those cytotoxic for MT-4 cells (Table 2).

Antiproliferative Activity. Due to the fact that some curcumin analogues showed antiproliferative activity against suspension cultures of lymphoid MT-4 cells at concentrations as low as 1.4 μM, we evaluated whether they were also capable of inhibiting the proliferation of cells (KB) derived from a solid human tumor, growing in monolayer (Table 2). Title compounds proved inhibitory against KB cells at concentrations comparable to those active against MT-4 cells, which ranged between 1.4 and 50 μM. In no case, however, did the potency of antiproliferative activity correlate with the presence of catechol groups, thus suggesting that test compounds inhibited cell proliferation by mechanisms different from the emergence of reactive quinone species.

Since some polyhydroxylated compounds active against IN, namely, flavones, have been reported to be topoisomerase inhibitors,[8] we investigated whether the antiproliferative activity of our IN inhibitors correlated with inhibition of cellular DNA binding proteins such as topo I and topo II. To this end we used an intact cell assay (see Experimental Section), rather than an in vitro enzyme assay, to take into account the capability of test compounds to penetrate the plasma membrane and to accumulate into the nuclear compartment. Etoposide (VP-16) and camptothecin (CPT) were used as reference drugs. As shown in Table 2, only compounds **7c** and **8b** were able to significantly increase the amount of protein-linked DNA breaks (PLDB) in KB cells, but again, no correlation could be found with either antiproliferative effect or activity against IN.

Selectivity of IN Inhibition in Enzyme Assays. The fact that our compounds active against IN were cytotoxic for cultured cell lines at concentrations significantly higher than those required for enzyme inhibition raised the possibility that they acted nonspecifically. In fact, a number of IN inhibitors have been reported to affect other viral enzymes in cell-free assays. Among them are ATA and flavones, which show a fairly similar structure−activity dependence for inhibition of both RT and IN.[8,24,25]

When evaluated for their capability to inhibit the recombinant HIV-1 RT and the cellular RNA polymerase II, none of the compounds were found active at 30 μM, the highest testable concentration (results not shown), thus suggesting that those compounds which turned out as potent IN inhibitors in enzyme assays exhibit a fairly high degree of selectivity.

Structure−Activity Relationships. The computational work was largely based on crystal structures retrieved from the CSD[17] of compounds strictly congeneric or coincident with those listed in Table 2. The crystal structures analyzed are reported in Table 3 together with their CSD identification code and values of relevant torsional angles. Model building and manipulation were realized using the SYBYL software package.[26] Computational protocols are detailed in the Experimental Section.

Conformations of structures containing a cinnamoyl moiety can be described through the torsional angles τ_1 and τ_2 defined in Figure 1. Owing to π-conjugation, τ_1 and τ_2 values close to 0° or 180° are associated with energetically stable planar arrangements. The importance of an extended planar conformation was first recognized by Burke et al.[9,27] who proposed 5,6- and 6,7-dihydroxynaphth-2-oyl nuclei (**14a**,**b**) as conformationally constrained mimetics of CAPE (**2**) and tyrphostin (**4**) analogues differing in the value of τ_1 (fixed to 0° in **14a** and to 180° in **14b**) (Chart 3). The 5,6-dihydroxy substitution pattern is associated with highest inhibitory activity when, in **14a**,**b**, R is different from OH (esters and amides). These data suggest that a conformation with a τ_1 value of about 0° is favored for interaction with IN.

The 3,4-dihydroxycinnamoyl moiety in Figure 1 becomes superimposable with that incorporated in the structures of quercetin (**1**) only if τ_2 takes a value of about 180° (X-ray coordinates of quercetin yield τ_1 and τ_2 values of 7.0° and −178.5°, respectively[28]). Contrary to quercetin, cyclovalone analogues **7a**−**f** display a relative orientation of the carbonyl defined by τ_2 values falling around 0°. This was inferred from crystal structures of congeners of **7a**−**c**,**f** exhibiting a total or nearly total coplanar arrangement about sp^2-hybridized atoms (kadmux, bzcptk20, and vabfin in Table 3). The remarkable inhibitory activities of the cyclovalone analogues bearing 3,4-dihydroxyls (**7b**−**f**) suggest that flexible cinnamoyl analogues likewise bind to IN with the carbonyl function oriented in syn with respect to the vinylic double bond (τ_2 value close to 0°). These data justify speculation that the binding modes of quercetin and cyclovalone analogues (**7b**−**f**) are different. Our

Table 3. Geometries Retrieved from the CSD of Compound Coincident or Congeneric with Those Listed in Table 2[a]

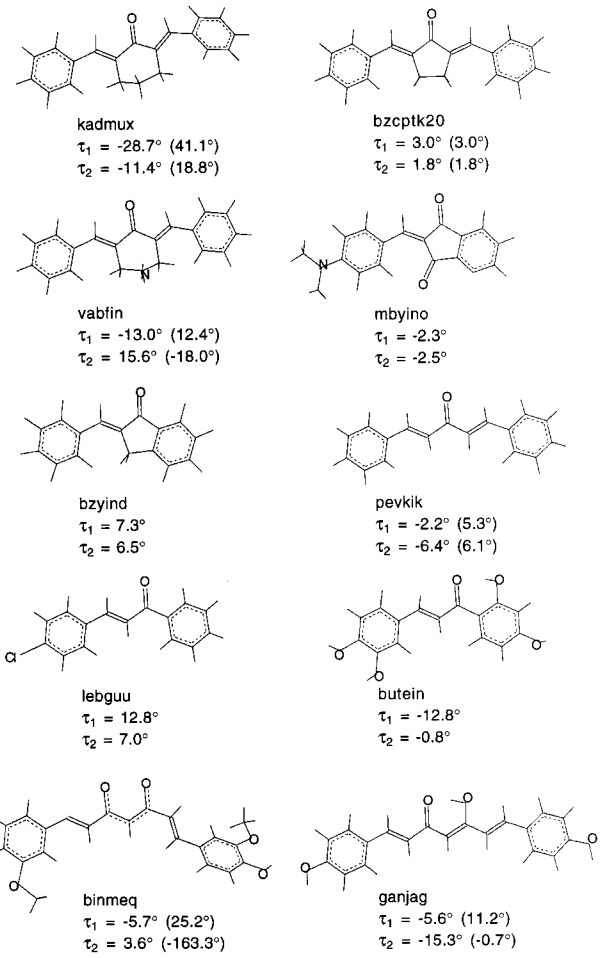

[a] The CSD reference code is given for each structure. τ_1 and τ_2 values are defined in Figure 1 (values in parentheses refer to the equivalent moiety oriented rightward). Cocrystallized species are not displayed for sake of clarity. Some structures lack one or more hydrogens.

hypothesis is supported by SARs reported for flavone derivatives.[8] Specifically, 3,4-dihydroxyflavone (**15a**) was found devoid of activity although it matches the general formula of Figure 1 with τ_2 fixed to about 180°. Additionally, baicalein (**15b**) proved to be active although it lacks the pharmacophoric 3,4-dihydroxycinnamoyl moiety.

Indan derivatives **8a**,**b**, inhibiting IN with different potency, are constrained in geometries very similar to those of cyclovalone analogues **7a**−**f** (see mbyino and bzyind in Table 3). It is not clear why the presence in **8b** of an endocyclic methylene in place of a carbonyl as in **8a** causes a 30-fold drop of activity. In fact, a strongly detrimental effect of the methylene is not entirely consistent with **7c** and **9c** being equipotent. Evidently, subtle steric and electrostatic effects come into play whose nature requires additional investigation to be elucidated.

Compounds **9a**−**d** and **10a**−**d** attain coplanar conformations judging from the X-ray structures of pevkik, legbuu, and butein in Table 3. It is worth noting the fairly good activity exhibited by **10d**, which features only a carbonyl and two catechol hydroxyls. To our knowledge this compound possesses the lowest number of

Chart 3. Naphthoic Acids (R═OH), Flavones, and AG593

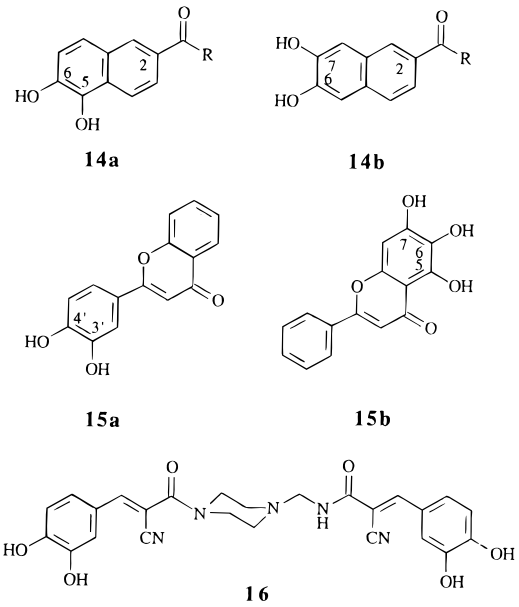

pharmacophoric heteroatoms (three) and is the smallest in size among the IN inhibitors structurally related to CAPE. A comparison of the IC_{50} values of **10a**,**b**,**d** suggests that the presence of the 2′-hydroxyl ortho to the carbonyl (**10b**) is responsible for a 20-fold drop of activity. Inspection of the crystal structures of **10b** (butein) reveals that the carbonyl oxygen is engaged in a hydrogen bond with the 2′-hydroxy group. Intramolecular hydrogen bond in **10b**, making the carbonyl oxygen less available to accept a hydrogen bond from IN, would account for the above results.

According to ^{1}H NMR measurements, curcumin (**3**) and **11a**−**d** exist exclusively as enolic tautomers (heptatrienolone structure). Our findings are in agreement with those reported by Sui et al. for dibenzoylcurcumin.[29] In the solid state curcumin (**3**) and its bisdesmethoxy derivative **11d** are enols displaying a planar conformation about at least one of the two cinnamoyl residues with a τ_2 value close to 0° (binmeq and ganjag, respectively, in Table 3). Provided that curcumin and **11b** inhibit IN in an extended coplanar arrangement mimicking that of cyclovalone analogues **7b**−**f**, there should be available a complementary cleft in the enzyme which is roughly flat in shape and of a size of approximately 20 × 7 Å (corresponding to the maximum length and width of **11b**). Our model contrasts with that proposed by Mazumder et al.,[11] who hypothesized that curcumin binds as a diketo tautomer in a folded conformation presenting the two phenyls stacked above each other, thus surrogating the catechol pattern commonly believed to be vital for activity. Moreover, Mazumder's model does not apply to **9b** which, like curcumin, is moderately active and bears the same substituents on the phenyl rings. In fact, conformational analyses, performed on **9b** using the SYBYL/SEARCH module, did not identify any folded conformation for this compound (results not shown). Taken together, these data suggest that intramolecular stacking of phenyl rings is not obligatory for bis-monohydroxylated inhibitors such as curcumin. Lack of free catechol hydroxyls, in curcumin as well as in compounds

9b and **12b**, can be nevertheless associated with moderate inhibitory activity (IC_{50} values ranging from 30 to 37 μM) thanks to other chemical functions favorably interacting with a flat "accessory" area of IN adjacent to the "pharmacophoric" binding site. Comparisons between curcumin and **11c** as well as between **9b** and **9d** suggest that one of the two *m*-methoxy groups in curcumin and **9b** might be involved in the above-hypothesized attractive interactions. The inactivity of **7a** indicates that a *m*-methoxy substituent must have a proper 3D orientation in order to exert a positive effect on potency (**7a** and **9b** share in fact the same bis-cinnamoyl substructure). Probably, the cyclohexanone skeleton in **7a** is not ideal for ensuring a full coplanarity of the two cinnamoyl moieties, whereas the less sterically encumbered backbone of **9b** can more easily allow both arylidene moieties to lie on the same plane. This view is suggested by inspection of the crystal structures of kadmux and pevkik as models of **7a** and **9b**, respectively.

Full coplanarity of the inhibitor structure is not an absolute requirement for high activity. In fact, computational studies performed in our laboratories established that certain IN inhibitors, such as AG593 (**16**),[12] cannot assume an entirely coplanar conformation (results not shown). Potency of tyrphostins has been reported to be poorly sensitive to the nature and the length of the linker between amide nitrogens,[12] suggesting that the linker is not part of the basic pharmacophore. An intramolecular loop may, in these cases, orient the terminal moieties into distinct binding sites, one of the two being complementary to the basic pharmacophore. The latter hypothesis was formulated earlier by Zhao et al.[27] who proposed the existence of two putative binding sites within IN, one being of "high affinity".

The 1,3-bis(cinnamoyl)benzene derivatives **12a**,**b** can access low-energy conformations entirely coplanar in which the C1−C(=O) and C3−C(=O) bonds of the 1,3-dicarbonylbenzene moiety are eclipsed with the benzene C2 atom. A substructure search in the CSD, using the central linker CO−C_6H_4−CO as a query, identified 13 out of 53 hits characterized by values of the torsional angles τ_3 (C2−C1−C=O) and τ_4 (C2−C3−C=O) within ±10°. The remaining 40 conformations were loosely clustered around the following pairs of τ_3 and τ_4 values: 0°/180°, 180°/0°, and 180°/180°. Using the SYBYL/SEARCH routine, we detected a low energy conformation for **12b** very similar to that proposed by Mazumder et al.[11] for curcumin (**3**). To sum up, flexibility of compounds **12a**,**b** does not allow a straightforward prediction of their bioactive conformations. We do not know whether these compounds, the largest in size of our series, fit partially or entirely into the flat "accessory" binding site.

The poor activity of the partially saturated ketone **13** (IC_{50} value can be estimated slightly above 100 μM) is likely related to disruption of coplanarity. Molecular mechanics calculations, performed on **13**, based on the Tripos force field,[30] revealed that the most stable conformations of this compound are folded so as to present the whole phenethyl chain out of the plane of the cinnamoyl unity. A transoid fully coplanar conformation of **13** was achieved at the cost of 4.9 kcal/mol of strain energy (difference with respect to the global minimum conformer). Attainment of a fully staggered conformation in CAPE (**2**), which also contains a phenethyl group, was penalized by only 1.7 kcal/mol of strain energy under the same computational settings. Twisting the terminal phenyl ring of about 90° in both **13** and CAPE lowered the internal energies to 3.2 and 0.0 kcal/mol, respectively. An overlay of these two "semiplanar" conformations about the common cinnamoyl frame shows two distinct locations for the terminal phenyl rings (Figure 3). Inactivity of **13** may in principle depend on an exceedingly high energetic cost to attain coplanarity. Alternatively, the phenyl ring in the semiplanar conformation of this compound may be sterically repelled upon binding.

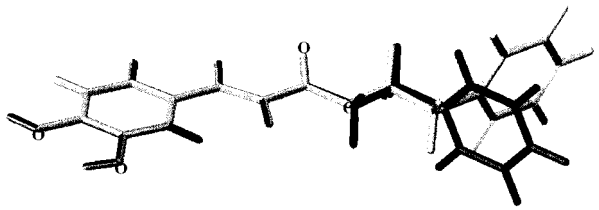

Figure 3. Molecular models of the inactive compound **13** (black) and the active CAPE (gray) overlayed about the common cinnamoyl residue. Conformations of **13** and CAPE are 3.2 and 0.0 kcal/mol higher in energy, respectively, than their corresponding global minimum conformers (Tripos force field). The terminal phenyl rings of the two compounds are not coincident in space.

Conclusions

Among the numerous polyhydroxylated compounds that have been shown to inhibit the HIV-1 IN in enzyme assays, very few of them are effective anti-HIV-1 agents when tested in cell-based assays. We therefore developed new IN inhibitors containing a cinnamoyl moiety with the C=C and C=O double bonds attaining a syn disposition (τ_2 about 0° in Figure 1). It was hoped that a backbone "frozen" in such a 3D arrangement, by geometrical or conformational constraints, could reduce cytotoxicity while retaining activity on infected cells.

In cell-free assays, our compounds inhibited neither the HIV-1 RT nor the cellular RNA polymerase II, thus suggesting that they specifically target the HIV-1 IN. Nevertheless, none of them were effective in preventing the HIV-1 multiplication in acutely infected cells. While this manuscript was in preparation, new data on curcumin analogues have been published[31] which are consistent with the above observations. Moreover, we have demonstrated that the antiproliferative potency of cinnamoyl-based structures, which does not correlate with the capability of inducing single-strand DNA breaks, occurs at concentrations up to 100 times higher than those effective against the viral enzyme. This suggests that in cell-based assays, cytotoxicity may not mask antiviral activity. Therefore, unless inhibition of cell proliferation is carried by title compounds through interaction with cell receptors on the plasma membrane, the possibility cannot be ruled out that the in vitro IN reaction fails to mimic the integration process occurring in the infected cells.

Examination of SARs developed from our compounds, interpreted in the light of crystallographic data and molecular modeling analyses, led to novel findings

concerning the molecular determinants of IN inhibitory activity within the class of cinnamoyl-containing structures. The importance of at least one catechol unit is suggestive of a binding mode similar to that of CAPE analogues. All these compounds are hypothesized to act in a conformation with the carbonyl group oriented in syn with respect to the vinylic double bond (τ_1 and τ_2 values of about 0° in Figure 1). This implies that the binding mode of the above inhibitors is different from that of flavone derivatives, such as quercetin, characterized by an anti disposition of the C=C−C=O moiety incorporated in the pyranone nucleus (τ_2 value of about 180°). Contrary to that hypothesized by Mazumder et al.,[11] we propose that bis-monohydroxylated inhibitors such as curcumin do not attain a folded conformation with the two phenyl rings stacking above each other. Lack of one of the two catechol hydroxyls, both crucial for high potency, may be compensated by the presence of other substructures which favorably interact with a flat "accessory" area of IN adjacent to the "pharmacophoric site". Lack of coplanarity in the inhibitor structure may abolish activity only if the out-of-plane moiety is oriented toward the steric boundaries of the binding site or a coplanar arrangement is associated with an exceedingly high strain energy.

Experimental Section

Chemistry. Melting points were determined on a Büchi 530 melting point apparatus and are uncorrected. Infrared (IR) spectra (Nujol mull) were recorded on a Perkin-Elmer 297 instrument. ^{1}H NMR spectra were recorded at 200 MHz on a Bruker AC 200 spectrometer using tetramethylsilane (Me_4Si) as internal reference. All compounds were routinely checked by TLC and ^{1}H NMR. TLC was performed by using aluminum-baked silica gel plates (Merck DC-Alufolien Kieselgel 60 F_{254}). Developed plates were visualized by UV light. Solvents were reagent grade and, when necessary, were purified and dried by standard methods. Concentration of solutions after reactions and extractions involved the use of a rotary evaporator operating at a reduced pressure of approximately 20 Torr. Organic solutions were dried over anhydrous sodium sulfate. Analytical results agreed to within ±0.40% of the theoretical values.

Syntheses. Specific examples presented below illustrate general synthetic procedures.

3,4-Bis(tetrahydropyran-2-yloxy)benzaldehyde. A solution of 3,4-dihydro-α-pyran (2.02 mL, 1.87 g, 22 mmol) in dichloromethane (12 mL) was added dropwise onto a well-stirred suspension of 3,4-dihydroxybenzaldehyde (1.0 g, 7.2 mmol) and pyridinium *p*-toluenesulfonate (0.04 g, 0.16 mmol) in the same solvent (34 mL). The mixture was stirred at room temperature for 1.5 h, then was washed with brine (3 × 50 mL), and dried. Evaporation of the solvent gave crude product which was purified by column chromatography on silica gel (cyclohexane/ethyl acetate, 9:2, as eluent) to obtain 3,4-bis-(tetrahydropyran-2-yloxy)benzaldehyde as a yellowish oil (1.1 g, 50% yield).

By this procedure were prepared the following compounds: 4-(tetrahydropyran-2-yloxy)benzaldehyde (100% yield, oil);[19] 2-hydroxy-4-(tetrahydropyran-2-yloxy)acetophenone (100% yield, mp 67−69 °C);[19] 4-(tetrahydropyran-2-yloxy)acetophenone (100% yield, mp 85−87 °C).[32]

2,6-Bis(3,4-dihydroxybenzylidene)cyclohexanone (7b). A mixture of 3,4-bis(tetrahydropyran-2-yloxy)benzaldehyde (3.1 g, 10.2 mmol), cyclohexanone (0.5 g, 5.1 mmol), and barium hydroxide octahydrate (4.8 g, 15.2 mmol) in methanol (100 mL) was stirred at 50 °C for 7 h. After cooling the solvent was evaporated, and the residue was treated with 1 M hydrochloric acid (100 mL) and extracted with ethyl acetate (3 × 50 mL). The organic layer was separated, washed with brine (3 × 100 mL), and dried. Evaporation of solvent furnished crude protected product which was suspended in methanol (40 mL) and treated with a catalytic amount of *p*-toluenesulfonic acid. After stirring at room temperature for 15 h the solvent was removed; the residue was treated with water and neutralized with a saturated solution of sodium hydrogen carbonate. The suspension was extracted with ethyl acetate (3 × 50 mL), and the organic extracts were collected, washed with brine (3 × 100 mL), and dried. Evaporation of the solvent gave crude product which was chromatographed on silica gel column (chloroform/methanol, 10:1, as eluent) to obtain pure **7b** (1.7 g, 99% yield).

This procedure was used for the synthesis of compounds **7c**−**e**, **8a,b**, **9c,d**, **10a**−**d**, **12a,b**, and **13** starting from 3,4-bis-(tetrahydropyran-2-yloxy)benzaldehyde (for reaction times at 50 °C and chromatographic systems, see Table 1) and for compounds **9a**,**b** starting from veratraldehyde and vanillic aldehyde, respectively; compound **7a** was obtained as reported previously.[33] Spectroscopic data for derivatives **7d**,**e**, **8b**, **9c**, **12a**,**b**, and **13** are reported below.

7d: IR cm^{-1} 3200 (OH) and 1580 (CO); ^{1}H NMR (DMSO-d_6) δ 4.86 (s, 4H, CH_2), 6.79−6.86 (m, 6H, benzene H), 7.49 (s, 2H, =CH-), 9.10 (br s, 4H, OH).

7e: IR cm^{-1} 3440, 3200 (OH), and 1570 (CO); ^{1}H NMR (DMSO-d_6) δ 3.95 (s, 4H, CH_2), 6.79−6.95 (m, 6H, benzene H), 7.45 (s, 2H, =CH-), 9.24 and 9.57 (2br s, 4H, OH).

8a: IR cm^{-1} 3440, 3200 (OH), and 1660 (CO); ^{1}H NMR (DMSO-d_6) δ 6.93 (d, J_o = 8.2 Hz, 1H, benzene C5−H), 7.67−7.93 (m, 6H, benzene C2−H, C6−H, and indan H), 8.38 (s, 1H, =CH-), 9.64 and 10.56 (2br s, 2H, OH).

9c: IR cm^{-1} 3460, 3250 (OH), and 1580 (CO); ^{1}H NMR (DMSO-d_6) δ 6.78 (d, J_o = 8.1 Hz, 2H, benzene C5−H), 6.99 (d, J_t = 15.9 Hz, 2H, C2−H and C4−H), 7.07 (d, J_o = 8.1 Hz, 2H, benzene C6−H), 7.14 (s, 2H, benzene C2−H), 7.56 (d, J_t = 15.9 Hz, 2H, C1−H and C5−H), 9.15 (br s, 4H, OH).

12a: IR cm^{-1} 3300 (OH) and 1640 (CO); ^{1}H NMR (DMSO-d_6) δ 6.83 (d, J_{o1} = 8.0 Hz, 2H, benzene C5−H), 7.23 (d, J_{o1} = 8.0 Hz, 2H, benzene C6−H), 7.31 (s, 2H, benzene C2−H), 7.68 (m, 5H, C2−H, C3−H, and benzoyl C5−H), 8.35 (d, J_{o2} = 7.7 Hz, 2H, benzoyl C4−H and C6−H), 8.65 (s, 1H, benzoyl C2−H), 9.19 and 9.78 (2br s, 4H, OH).

12b: IR cm^{-1} 3300 (OH) and 1635 (CO); ^{1}H NMR (DMSO-d_6) δ 6.86 (d, J_{o1} = 8.5 Hz, 4H, benzene C3−H and C5−H), 7.71−7.82 (m, 9H, C2−H, C3−H, benzene C2−H, C6−H, and benzoyl C5−H), 8.38 (d, J_{o2} = 7.7 Hz, 2H, benzoyl C4−H and C6−H), 8.68 (s, 1H, benzoyl C2−H), 10.20 (br s, 2H, OH).

13: IR cm^{-1} 3480, 3160 (OH), and 1630 (CO); ^{1}H NMR (DMSO-d_6) δ 2.86−2.98 (m, 4H, CH_2), 6.58 (d, J_t = 16.1 Hz, 1H, C2−H), 6.77 (d, J_o = 8.0 Hz, 1H, hydroxybenzene C5−H), 7.01 (d, J_o = 8.0 Hz, 1H, hydroxybenzene C6−H), 7.07 (s, 1H, hydroxybenzene C2−H), 7.15−7.30 (m, 5H, benzene H), 7.47 (d, J_t = 16.1 Hz, 1H, C3−H), 9.15 and 9.60 (2br s, 2H, OH).

3,5-Bis(3,4-dihydroxybenzylidene)-4-piperidone Hydrochloride (7f). A solution of 4-piperidone hydrate hydrochloride (1.0 g, 6.5 mmol) in glacial acetic acid (40 mL) was saturated with anhydrous hydrogen chloride and then treated with a suspension of 3,4-dihydroxybenzaldehyde (2.7 g, 19.5 mmol) in the same solvent (50 mL). After stirring at room temperature for 48 h the precipitate which formed was filtered and washed with water, ethanol, and light petroleum ether, in turn, to obtain pure **7f** (2.2 g, 92% yield).

1,7-Bis(4-hydroxyphenyl)-1,6-heptadiene-3,5-dione (11c). A solution of 4-hydroxybenzaldehyde (2.4 g, 19.8 mmol) and acetylacetone (1.0 g, 9.9 mmol) in *N*,*N*′-dimethylformamide (2 mL) was treated with boric acid (2.0 g, 32.0 mmol), and the mixture was heated at 100 °C for 5 min. After this time a solution of 1,2,3,4-tetrahydroquinoline (2.0 mL, 2.1 g, 15.8 mmol) and acetic acid (0.6 mL) in *N*,*N*′-dimethylformamide (2 mL) was added. The resulting mixture was heated at 100 °C for 4 h, then cooled, diluted with 20% acetic acid (100 mL), and stirred at room temperature for 1 h. The precipitate which formed was filtered, washed with ethyl acetate and then with light petroleum ether, and finally chromatographed to afford pure **11c** (790 mg, 26% yield).

By this procedure were prepared compounds **11a**,**b**,**d** (for chromatographic systems, see Table 1); oily derivatives **11a**,**d** were extracted with ethyl acetate before chromatographic purification. Spectroscopic data of these derivatives together with IR and ^{1}H NMR spectra of curcumin (**3**) are reported below. The presence of a singlet (1H) for C4−H in the ^{1}H NMR spectra of curcumin (**3**), **11b**,**c**, and **11a**,**d** (δ = 5.94, 6.08, 6.04, 5.82, and 5.86 ppm, respectively), accounts for the heptatrienolone structure.

3: IR cm^{-1} 3300 (OH) and 1620 (CO); ^{1}H NMR (CD_3OD) δ 3.90 (s, 6H, OCH_3), 5.94 (s, 1H, C4−H), 6.62 (d, J_t = 15.8 Hz, 2H, C2−H and C6−H), 6.81 (d, J_o = 8.0 Hz, 2H, benzene C5−H), 7.09 (d, J_o = 8.0 Hz, 2H, benzene C6−H), 7.19 (s, 2H, benzene C2−H), 7.56 (d, J_t = 15.8 Hz, 2H, C1−H and C7−H).

11a: IR cm^{-1} 1610 (CO); ^{1}H NMR ($CDCl_3$) δ 3.92 and 3.94 (2s, 12H, OCH_3), 5.82 (s, 1H, C4−H), 6.49 (d, J_t = 15.6 Hz, 2H, C2−H and C6−H), 6.87 (d, J_o = 8.0 Hz, 2H, benzene C5−H), 7.09 (d, J_m = 1.9 Hz, 2H, benzene C2−H), 7.16 (d, J_o = 8.0 Hz, J_m = 1.9 Hz, 2H, benzene C6−H), 7.60 (d, J_t = 15.6 Hz, 2H, C1−H and C7−H), 15.80 (br s, 1H, OH).

11b: IR cm^{-1} 3300 (OH) and 1590 (CO); ^{1}H NMR (DMSO-d_6) δ 6.08 (s, 1H, C4−H), 6.58 (d, J_t = 15.8 Hz, 2H, C2−H and C6−H), 6.78 (d, J_o = 8.1 Hz, 2H, benzene C5−H), 7.02 (d, J_o = 8.1 Hz, 2H, benzene C6−H), 7.08 (s, 2H, benzene C2−H), 7.46 (d, J_t = 15.8 Hz, 2H, C1−H and C7−H), 8.71, 9.22, and 9.69 (3br s, 5H, OH).

11c: IR cm^{-1} 3300 (OH) and 1620 (CO); ^{1}H NMR (DMSO-d_6) δ 6.04 (s, 1H, C4−H), 6.71 (d, J_t = 15.8 Hz, 2H, C2−H and C6−H), 6.82 (d, J_o = 8.5 Hz, 4H, benzene C3−H and C5−H), 7.51−7.60 (m, 6H, C1−H, C7−H, benzene C2−H, and C6−H), 10.10 (br s, 3H, OH).

11d: IR cm^{-1} 1610 (CO); ^{1}H NMR ($CDCl_3$) δ 5.85 (s, 1H, C4−H), 6.63 (d, J_t = 15.6 Hz, 2H, C2−H and C6−H), 7.38 (m, 6H, benzene C3−H, C4−H, and C5−H), 7.57 (m, 4H, benzene C2−H and C6−H), 7.67 (d, J_t = 15.6 Hz, 2H, C1−H and C7−H), 15.90 (br s, 1H, OH).

Molecular Modeling. The October 1996 and April 1997 releases (3D graphics 5.12 and 5.13 versions for UNIX platforms) of the CSD[17] were searched through substructure queries using the CSD/QUEST graphical routine. Molecular modeling was performed with use of the software package SYBYL[26] running on a Silicon Graphics Indigo XS24 workstation. Molecular models of compounds **13** and CAPE (**3** in Chart 1), whose coordinates were not available from the CSD, were assembled using standard bond lengths and bond angles of the SYBYL fragment library. Conformational energies were calculated according to the molecular mechanics Tripos force field[30] including electrostatics. Partial atomic charges were assigned using the Gasteiger−Hückel method.[34,35] Geometry optimizations were performed with the SYBYL/MAXIMIN2 minimizer by applying the Broyden−Fletcher−Goldfarb−Shanno algorithm[36] and setting an energy difference of 0.001 kcal/mol as convergence criterion. Structures of compound **13** and CAPE were superimposed by minimizing the root-mean-square distance between the non-hydrogen atoms of the cinnamoyl moiety using the SYBYL/FIT command. Conformational analyses on **9b**, **12b**, **13**, **16**, and CAPE were carried out using the SYBYL/SEARCH module. Properly selected torsional angles were scanned by 20° increments throughout 0−340°, or 0−160° for symmetrically substituted phenyl rings. A van der Waals scaling factor of 0.75 was applied to "soften" steric contacts. Such scaling was aimed at minimizing the typical limitation of systematic rigid search consisting of lack of relaxation for each conformation. The number of output conformations to be examined was reduced by setting the "energy window" (energy difference between the generated conformation and the current minimum) to 10.0 kcal/mol. Results from conformational analyses were evaluated by means of the SYBYL/MOLECULAR SPREADSHEET routine. Differences in energies between conformations, as in the modeling of **13** and CAPE, were computed on geometry-optimized structures.

Integrase and DNA Substrates. Expression of the HIV-1 IN protein with an amino-terminal polyhistidine tag was obtained by IPTG induction of the *E. coli* strain BL21(DE3) containing the pINSD·His vector. Protein purification was carried out following the Novagen procedure, except for the presence of 5 mM CHAPS in binding buffer (5 mM imidazole, 0.5 M NaCl, 20 mM Tris-HCl, pH 7.9), washing buffer (60 mM imidazole, 0.5 M NaCl, 20 mM Tris-HCl, pH 7.9), and elute buffer (1 M imidazole, 0.5 M NaCl, 50 mM Tris-HCl, pH 7.9, 5 mM β-mercaptoethanol).

The following oligos representing the terminal 21 nucleotides of the HIV-1 U5 LTR were used in this study: **A**, 5′-GTG TGG AAA ATC TCT AGC AGT-3′ (plus strand); **B**, 5′-ACT GTC AGA GAT TTT CCA CAC-3′ (minus strand); **C**, 5′-GTG TGG AAA ATC TCT AGC A-3′ (plus strand two nucleotides shorter than **A**). For standard 3′-processing assays, **C** was annealed with **B** in 0.1 M NaCl by heating at 80 °C and slowly cooling to room temperature overnight. This double-stranded substrate was labeled by introducing at the 3′-end of **C** the two missing nucleotides using [α-^{32}P]dGTP, cold dTTP, and Klenow polymerase. Unincorporated [α-^{32}P]-dGTP was separated from the duplex substrate by two consecutive runs through G-25 Sephadex quick spin columns. Alternatively, **C** was labeled at the 5′-end using [γ-^{32}P]ATP and T4 polynucleotide kinase, purified through G-25 Sephadex quick spin column, and then annealed with unlabeled **B** in 0.1 M NaCl as stated above. ATA, used as a standard in our IN assays, was purchased from Aldrich (12,326.9; batch 68853-104).

3′-Processing Assay. Standard reaction conditions were 40 mM NaCl, 10 mM $MnCl_2$, 25 mM Tris-HCl, pH 7.5, 1 mM DTT, 2% glycerol, 1 nM duplex **B:C** labeled at the 3′-end, 5 nM IN (considered as monomer). Incubation was carried out at 37 °C for 30 min in a volume of 50 μL. The reaction was stopped by adding an equal volume of 0.5 M Na_2HPO_4. Each sample (90 μL) was added to a well of a Multiscreen 96-well filtration plate preloaded with 100 μL of DEAE Sephacel slurry (equilibrated in 0.5 M Na_2HPO_4) which had been vacuum-dried. Vacuum was applied after incubation at room temperature for 10 min. The uncleaved, labeled substrate was retained in the resin, whereas labeled dinucleotide (GT) products were collected at the bottom of 96-well filtration plates and counted for radioactivity. When reactions were analyzed by denaturing PAGE, 6 μL of each sample was taken before stopping the reaction and added to 3 μL of sample buffer (96% formamide, 20 mM EDTA, 0.08% bromophenol blue, 0.25% xylene cyanol). Samples were heated at 100 °C for 3 min, layered onto a denaturing 15% polyacrylamide gel (7 M urea, 0.09 M Tris borate, pH 8.3, EDTA 2 mM, 15% acrylamide), and run for 1 h at 65 W. Reaction products were visualized by autoradiography and quantified by densitometric analysis.

Biological Assays. Compounds were solubilized in DMSO at 200 mM and then further diluted. MT-4 cells were grown at 37 °C in a 5% CO_2 atmosphere in RPMI 1640 medium supplemented with 10% fetal calf serum (FCS), 100 IU/mL penicillin G, and 100 μg/mL streptomycin. Cell cultures were checked periodically for the absence of mycoplasma contamination with a MycoTect Kit (Gibco). HIV-1 stock solutions had titers of 4.5 × 10^6 50% cell culture infectious dose ($CCID_{50}$)/mL. Cytotoxicity evaluation was based on the viability of mock-infected cells, as monitored by the MTT method. Activity of the compounds against the HIV-1 multiplication in acutely infected cells was based on inhibition of virus-induced cytopathic effect in MT-4 cells and was determined by the 3-(4,5-dimethylthiazol-1-yl)-2,5-diphenyltetrazolium bromide (MTT) method.[37] Anti-RNA polymerase II assays were performed as previously described.[38] Purified rRT was assayed for its RNA-dependent polymerase-associated activity in a 50-μL volume containing 50 mM Tris-HCl (pH 7.8), 80 mM KCl, 6 mM $MgCl_2$, 1 mM DTT, 0.1 mg mL^{-1} BSA, 0.5 OD_{260} unit mL^{-1} template: primer [poly(rC)·oligo$(dG)_{12-18}$], and 10 μM [^{3}H]dGTP (1 Ci mmol^{-1}). After incubation for 30 min at 37 °C, the samples were spotted on glass fiber filters (Whatman GF/A), and the acid-insoluble radioactivity was determined.

Quantitation of Protein-Linked DNA Breaks. A modi-

fied in vivo K-SDS coprecipitation assay[39] was used for quantification of protein-linked DNA breaks (PLDB) levels. Briefly, KB cells were seeded at a density of 2.5×10^5/mL and labeled with [^{14}C]thymidine (0.75 μCi/mL) for 48 h. Monolayers were washed twice, and after trypsinization, cells were resuspended in aliquots of 3×10^5/mL and were incubated for 1 h at 37 °C. Then, duplicate samples were treated with test drugs at concentrations 10 times higher than respective CC_{50} values and further incubated for 1 h. Cells were collected by centrifugation at 2000*g* for 10 min and resuspended in 1 mL of warm lysis buffer (1.5% SDS, 5 mM EDTA, 0.4 mg/mL salmon sperm DNA), and the viscous cell lysates were sheared by passage through a 22-gauge needle five times. After 10-min incubation at 65 °C, KCl was added to a final concentration of 100 mM; samples were chilled in an ice bath for 10 min and centrifuged at 3500*g* for 10 min at 4 °C. Pellets were resuspended in 1 mL of warm washing buffer (10 mM Tris-HCl, pH 8.0, 100 mM KCl, 1 mM EDTA, 0.1 mg/mL salmon sperm DNA) and again incubated for 10 min at 65 °C, chilled in an ice bath, and centrifuged as above. After a second washing step, pellets were solubilized at 65 °C in 400 μL of water and counted for radioactivity.

Acknowledgment. The authors thank Italian Ministero della Sanità-Istituto Superiore di Sanità-IX Progetto AIDS 1996 (Grants 9403-07 and 9403-59) for financial aid. Thanks are also due to Foundation "Istituto Pasteur - Fondazione Cenci Bolognetti", University of Rome "La Sapienza" (Italy), Assessorato Igiene Sanità, Regione Sardegna, and MURST (Rome) for partial support.

References

(1) Artico, M. Nonnucleoside anti-HIV-1 Reverse Transcriptase Inhibitors (NNRTIs): A Chemical Survey from Lead Compounds to Selected Drugs for Clinical Trials. *Farmaco* **1996**, *51*, 305−331.

(2) Appelt, K.; Clare, M.; Pettit, S. C.; Michael, S. F.; Swanstrom, R.; Moore, M. C.; Dreyer, G. B.; Erickson, J. W. Therapeutic Approaches to HIV. *Perspect. Drug Discovery Des.* **1993**, *1*, 23−128.

(3) De Clercq, E. Toward Improved anti-HIV Chemotherapy: Therapeutic Strategies for Intervention with HIV Infections. *J. Med. Chem.* **1995**, *38*, 2491−2517.

(4) La Femina, R. L.; Schneider, C. L.; Robbins, H. L.; Callahan, P. L.; LeGrow, K.; Roth, E.; Schleif, W. A.; Emini, E. A. Requirement of Active Human Immunodeficiency Virus Type 1 Integrase Enzyme for Productive Infection of Human T-Lymphoid Cells. *J. Virol.* **1992**, *66*, 7414−7419.

(5) Sakai, H.; Kawamura, M.; Sakuragi, J.; Sakuragi, S.; Shibata, R.; Ishimoto, A.; Ono, N.; Ueda, S.; Adachi, A. Integration is Essential for Efficient Gene Expression of Human Immunodeficiency Virus type 1. *J. Virol.* **1993**, *67*, 1169−1174.

(6) Brown, P. O.; Bowerman, B.; Varmus, H. F.; Bishop, J. M. Retroviral Integration: Structure of the Initial Covalent Product and its Precursor, and a Role for the Viral Integrase Protein. *Proc. Natl. Acad. Sci. U.S.A.* **1989**, *86*, 2525−2529.

(7) Bushman, F. D.; Fujiwara, T.; Craigie, R. Retroviral DNA Integration Directed by HIV Integration Protein in Vitro. *Science* **1990**, *249*, 1555−1558.

(8) Fesen, M. K.; Pommier, Y.; Leteurtre, F.; Hiroguchi, S.; Young, J.; Kohn, K. W. Inhibition of HIV-1 Integrase by Flavones, Caffeic Acid Phenethyl Ester (CAPE) and Related Compounds. *Biochem. Pharmacol.* **1994**, *48*, 595−608.

(9) Burke, T. R., Jr.; Fesen, M. R.; Mazumder, A.; Wang, Y.; Carothers, A. M.; Grunberger, D.; Driscoll, J.; Khon, K.; Pommier, Y. Hydroxylated Aromatic Inhibitors of HIV-1 Integrase. *J. Med. Chem.* **1995**, *38*, 4171−4178.

(10) LaFemina, R. L.; Graham, P. L.; LeGrow, K.; Hastings, J. C.; Wolfe, A.; Young, S. D.; Emini, E. A.; Hazuda, D. J. Inhibition of Human Immunodeficiency Virus Integrase by Bis-Catechols. *Antimicrob. Agents Chemother.* **1995**, *39*, 320−324.

(11) Mazumder, A.; Raghavan, K.; Weistein, J.; Kohn, K. W.; Pommier, Y. Inhibition of Human Immunodeficiency Virus Type-1 Integrase by Curcumin. *Biochem. Pharmacol.* **1995**, *49*, 1165−1170.

(12) Mazumder, A.; Gazit, A.; Levitzki, A.; Nicklaus, M.; Yung, J.; Kohlhagen, G.; Pommier, Y. Effects of Tyrphostins, Protein Kinase Inhibitors, on Human Immunodeficiency Virus Type 1 Integrase. *Biochemistry* **1995**, *34*, 15111−15122.

(13) Eich, E.; Pertz, H.; Kaloga, M.; Schultz, J.; Fesen, M. R.; Mazumder, A.; Pommier, Y. (−)-Arctigenin as a Lead Structure for Inhibitors of Human Immunodeficiency Virus Type-1 Integrase. *J. Med. Chem.* **1996**, *39*, 86−95.

(14) Robinson, W. E., Jr.; Reinecke, M. G.; Abdel-Malek, S.; Jia, Q.; Chow, S. A. Inhibitors of HIV-1 Replication that Inhibit HIV Integrase. *Proc. Natl. Acad. Sci. U.S.A.* **1996**, *93*, 6326−6331.

(15) Li, C. J.; Zhang, L. J.; Dezube, B. J.; Crumpacker, C. S.; Pardee, A. B. Three Inhibitors of Type 1 Human Immunodeficiency Virus Long Terminal Repeat-Directed Gene Expression and Virus Replication. *Proc. Natl. Acad. Sci. U.S.A.* **1993**, *90*, 1839−1842.

(16) Dyda, F.; Hickman, A. B.; Jenkins, T. M.; Engelman, A.; Craigie, R.; Davies, D. R. Crystal Structure of the Catalytic Domain of HIV-1 Integrase: Similarity to Other Polynucleotidyl Transferases. *Science* **1994**, *266*, 1981−1986.

(17) Bernstein, F. C.; Koetzle, T. F.; Williams, G. J. B.; Meyer, E. F., Jr.; Brice, M. D.; Rodgers, J. R.; Kennard, O.; Shimanouchi, T.; Tasumi, T. The Protein Data Bank: A Computer Based Archival File for Macromolecular Structures. *J. Mol. Biol.* **1977**, *112*, 535−542.

(18) Babu, K. V. D.; Rajasekharan, K. N. Simplified Condition for Synthesis of Curcumin I and Other Curcuminoids. *OPPI Briefs* **1994**, *26*, 674−677.

(19) Severi, F.; Costantino, L.; Benvenuti, S.; Vampa, G.; Mucci, A. Synthesis and Description of Chalcone-like Compounds, Inhibitors of Aldose Reductase. *Med. Chem. Res.* **1996**, *6*, 128−136.

(20) Oosawa, T.; Ochi, H. Jpn. Kokai Tokkyo Koho JP 07,206,763 [95,206,753]; *Chem. Abstr.* **1996**, *124*, 8511s.

(21) Zhao, H.; Neamati, N.; Mazumder, A.; Sunder, S.; Pommier, Y.; Burke, T. R., Jr. Arylamide Inhibitors of HIV-1 Integrase. *J. Med. Chem.* **1997**, *40*, 1186−1194.

(22) Cushman, M.; Sherman, P. Inhibition of HIV-1 Integration Protein by Aurintricarboxylic Acid Monomers, Monomer Analogues and Polymer Fractions. *Biochem. Biophys. Res. Commun.* **1992**, *185*, 85−90.

(23) Engelman, A.; Mizouchi, K.; Craigle, R. HIV-1 DNA Integration Mechanism of Viral DNA Cleavage and DNA Strand Transfer. *Cell* **1991**, *67*, 1211−1221.

(24) Ono, K.; Nakane, H.; Fukushima, M.; Chermann, J.-C.; Barré-Sinoussi, F. Differential Inhibitory Effects of Various Flavonoids on the Activities of Reverse Transcriptase and Cellular DNA and RNA Polymerases. *Eur. J. Biochem.* **1990**, *190*, 469−476.

(25) Chu, S. C.; Hsiech, Y. S.; Lin, J. Y. Inhibitory Effects of Flavonoids on Moloney Murine Leukemia Virus Reverse Transcriptase Activity. *J. Nat. Prod.* **1992**, *55*, 179−183.

(26) SYBYL Molecular Modeling System (version 6.2), Tripos Assoc., St. Louis, MO.

(27) Zhao, H.; Neamati, N.; Hong, H.; Mazumder, A.; Wang, S.; Sunder, S.; Milne, G. W. A.; Pommier, Y.; Burke, T. R., Jr. Coumarin-Based Inhibitors of HIV-1 Integrase. *J. Med. Chem.* **1997**, *40*, 242−249.

(28) Rossi, M.; Rickles, L. F.; Halpin, W. A. The Crystal and Molecular Structure of Quercetin: a Biologically Active and Naturally Occurring Flavonoid. *Bioorg. Chem.* **1986**, *14*, 55−69.

(29) Sui, Z.; Salto, R.; Li, J.; Craik, C.; Ortiz de Montellano, P. R. Inhibition of the HIV-1 and HIV-2 Proteases by Curcumin and Curcumin Boron Complexes. *Bioorg. Med. Chem.* **1993**, *1*, 415−422.

(30) Clark, M.; Cramer, R. D., III; Van Opdenbosch, N. Validation of the General Purpose Tripos 5.2 Force Field. *J. Comput. Chem.* **1989**, *10*, 982−1012.

(31) Mazumder, A.; Neamati, N.; Sunder, S.; Schulz, J.; Pertz, H.; Eich, E.; Pommier, Y. Curcumin analogues with altered potencies against HIV-1 integrase as probes for biochemical mechanisms of drug action. *J. Med. Chem.* **1997**, *40*, 3057−3063.

(32) Burckhalter, J. H.; Dixon, W. D.; Black, M.; Westland, R. D.; Werbel, L. M.; DeWald, H. A.; Dice, J. R.; Rodney, G.; Kaump, D. H. 2-(2-Pyridyl)-1,2-diaryl Alkanols as Hypocholesteremic Agents. *J. Med. Chem.* **1967**, *10*, 565−575.

(33) Samdahl, B. Diveratrylidene and Divanillydene Compounds of Cyclohexanone, Comprising Several New Indicators. *J. Pharm. Chim.* **1928**, *7*, 162−173.

(34) Gasteiger, J.; Marsili, M. Iterative Partial Equalization of Orbital Electronegativity. *Tetrahedron* **1980**, *36*, 3219−3228.

(35) Purcel, V. P.; Singer, J. A. A Brief Review and Table of Semiepirical Parameters Used in the Hückel Molecular Orbital Method. *J. Chem. Eng. Data* **1967**, *12*, 235−246.

(36) Head, J.; Zerner, M. C. A Broyden-Fletcher-Goldfarb-Shanno Optimization Procedure for Molecular Geometries. *Chem. Phys. Lett.* **1985**, *122*, 264−274.

(37) Pauwels, R.; Balzarini, J.; Baba, M.; Snoeck, R.; Schols, D.; Herdewijn, P.; Desmyster, J.; De Clercq, E. Rapid and Automated Tetrazolium-Based Assay for the Detection of anti-HIV Compounds. *J. Virol. Methods* **1988**, *20*, 309−321.

(38) Tomassini, J.; Davies, M. E.; Amstrong, M. E.; Hastings, J.; Hazuda, D.; Lewis, J.; McClemens, W.; Wolfe, A.; Selnick, H.; Baldwin, J.; Bourgeois, M.; Ponticello, G.; Radilowski, E.; Smith, G.; Tebben, A. Inhibition of the cap-dependent endonuclease of influenza virus by 4-substituted-2,4-dioxobutanoic acid compounds. *Antimicrob. Agents Chemother.* **1994,** *38*, 2827−2837.
(39) Lee, K. H.; Imakura, Y.; Haurna, M.; Beers, S. A.; Thurston, L. S.; Dai, H. J.; Chen, C. H. Antitumor Agent 107. New Cytotoxic 4-Alkylamino Analogues of 4′-Demethyl-epipodophyllotoxin as Inhibitors of Human DNA Topoisomerase II. *J. Nat. Prod.* **1989**, *52*, 606−613.
(40) Samdahl, B. Some New Indicators, Derivatives of Cyclohexanone. *J. Pharm. Chim.* **1930**, *11*, 8−19.
(41) Samdhal, B.; Hansen, B. Condensation of Cyclopentanone with Phenol Aldehydes. *J. Pharm. Chim.* **1928**, *7*, 162−173.
(42) Ionescu, M. V. New Reaction for Aromatic Aldehydes. *Bull. Soc. Chim.* **1930**, *47*, 210−214.
(43) Haworth, R. D.; Lamberton, A. H. Some Derivatives of Catechol and Pyrogallol. II. *J. Chem. Soc.* **1946**, 1003−1005.
(44) Glaser, E.; Tramer, E. Condensation Product of Vanillin and Salicylaldehyde with Acetone and the Mechanism of this Condensation. *J. Prakt. Chem.* **1927**, *116*, 331−346.
(45) McGookin, A.; Sinclair, D. J. Isomerism of the Styryl Alkyl Ketones. IV. 4-Hydroxy- and some Derivatives of 2-Hydroxystyryl Alkyl Ketones. *J. Chem. Soc.* **1928**, 1170−1177.
(46) Klinke, P.; Gibian, H. Chalcones. *Chem. Ber.* **1961**, *94*, 26−38.
(47) Dziedzic, S. Z.; Hudson, B. J. F. Polyhydroxy Chalcones and Flavanones as Antioxidants for Edible Oils. *Food Chem.* **1983**, *12*, 205−212.
(48) Geissman, T. A.; Clinton, R. O. Flavanones and Related Compounds. I. The Preparation of Polyhydroxychalcones and Flavanones. *J. Am. Chem. Soc.* **1946**, *68*, 697−700.
(49) Jentzsch, K.; Spiegel, P.; Kamitz, R. Qualitative and Quantitative Studies of Curcuma Dyes in Different Zingiberaceae Drugs. 2. Quantitative studies. *Sci. Pharm.* **1970**, *38*, 50−58.
(50) Pabon, H. J. J. A Synthesis of Curcumin and Related Compounds. *Recl. Trav. Chim. Pays Bas* **1964**, *83*, 379−386.

JM9707232